Photoluminescence study of AlGaAs/GaAs quantum wells grown by molecular beam epitaxy with in-situ / ex–situ growth interruptions

P. Acosta-Díaz, O. Cano-Aguilar and F.L. Castillo-Alvarado
Physics Department, Escuela Superior de Física y Matemáticas del IPN, Unidad Profesional "Adolfo López Mateos", México, D.F., México.

M. Meléndez-Lira and M. López-López*
Physics Department, Centro de Investigación y Estudios Avanzados del IPN, Apartado Postal 14-470, México 07000 D.F., México.

The specific properties of quantum wells (QWs) grown by molecular beam epitaxy (MBE) are directly affected by several aspects, such as non-intentional incorporated impurities, alloy disorder, interface roughness, etc. These aspects strongly depend on the particular process used during the MBE growth. In this work, we present results of a photoluminescence spectroscopy (PL) study of $Al_xGa_{1-x}As$ / GaAs QWs grown by MBE on GaAs buffer layers which were processed by ex-situ or in-situ growth interruptions. The QWs exhibit drastic changes in their PL spectra depending on the type of interruption process performed on the GaAs buffer layer surface. Roughness at the QWs interfaces has been calculated and correlated with the growth interruption process.

Keywords: Quantum wells, molecular beam epitaxy, growth interruption, in-situ processing.

Las propiedades especificas de pozos cuánticos crecidos por epitaxia de haces moleculares (EHM) se ven directamente afectadas por diversos factores tales como: incorporación no intencional de impurezas, desorden en las aleaciones, rugosidad en las interfaces, etc. Estos aspectos dependen fuertemente del proceso particular usado durante el crecimiento por EHM. En este trabajo presentamos los resultados de un estudio realizado por espectroscopia de fotoluminiscencia (FL) de pozos cuánticos de AlGaAs/GaAs crecidos por EHM sobre capas colchón de GaAs las cuales fueron procesadas con interrupciones in-situ o ex-situ en el crecimiento. Los pozos cuánticos mostraron cambios drásticos en sus espectros de FL que dependen del tipo de proceso de interrupción realizado en la capa colchón de GaAs. Se calculó la rugosidad en las interfaces de los pozos cuánticos y se correlacionó con los procesos de interrupción del crecimiento.

Descriptores: Pozos cuánticos, epitaxia por haces moleculares, interrupción del crecimiento, procesamiento in-situ.

1. Introduction

Nowadays the use of "quantum devices" based on compound semiconductors has caused a great impact on our daily life. A lot of progress has been made in the growth technology of these materials since the invention of molecular-beam epitaxy (MBE) in the late 1960's.

The III-V semiconductor compounds are the most commonly employed materials in the fabrication of such devices, among which GaAs and $Al_{1-x}Ga_xAs$ play an important role. This importance has been reflected in a very good knowledge of the properties of these materials, and the intense and continuous study to improve growing and processing methods in order to obtain high quality quantum-well heterostructures (QWH's). High quality refers to smooth interfaces, few non-intentional incorporated impurities and high photoluminescence efficiency.

One of the most important problems related with growth of QWH's is the structural disorder at atomic scale, which occurs at the AlGaAs/GaAs interfaces of the heterostructure, usually called "interface roughness" [1,2]. The control of the interface quality in AlGaAs/GaAs QWs is important in order to realize an ideal two-dimensional (2D) exciton gas. Photoluminescence spectroscopy (PL) is very sensitive to the microscopic interfacial structure of AlGaAs/GaAs QWs [3,4]. There are many reports of the interfacial roughness in AlGaAs/GaAs QWs fabricated by MBE and studied by PL [5-7]. In particular, the effects of growth interruptions on the QWs luminescence have been the subject of intense research [8-10]. By applying growth interruption techniques it is possible to prepare QWs with islands at the AlGaAs/GaAs interfaces consisting of atomically flat terraces comparable with or even larger than the exciton Bohr radius. The smoothness of the terraces at the interfaces within 1 monolayer (ML) of GaAs eliminates the contribution of ML thickness fluctuations to the broadening of exciton emission. Thus, PL spectra from samples with growth interruption at the interfaces are narrower than those without it [8].

In all the previous studies, the growth interruption was performed inside the MBE chamber by closing the shutters of Ga and Al sources, thus minimizing the non-intentional incorporation of impurities. However, growth interruptions before the deposition of QWs are also necessary for other purposes. For example, during the in-situ processing of GaAs for the fabrication of low dimensional structures, MBE growth is interrupted and GaAs wafers have to be transferred to different ultra-high vacuum (UHV) chambers through UHV-tunnels [11,12]. Other applications require growth interruptions for an ex-situ photolithography, this step involves exposure to air of the GaAs surface [13].

*Corresponding author, e-mail: mlopez@fis.cinvestav.mx

Table 1. Characteristics of the studied samples

Sample Number	Characteristics	Buffer layer thickness (Å)	Surface reconstruction*	Interruption process
0	Reference	5000		None
1	*Ex-situ* processed	5000	2x4	Air exposure (30 min)
2	*Ex-situ* processed	500	2x4	Air exposure (30 min)
3	*In-situ* processed	130	2x4	3 hrs in UHV ($1x10^{-9}$ Torr)
4	*In-situ* processed	130	4x4	3 hrs in UHV ($1x10^{-9}$ Torr)

* During growth interruption

The study of the effects of the in-situ/ex-situ growth interruption on the properties of the QWs is important to evaluate possible damages caused by these steps.

In this work, we used PL to study the properties of growth interrupted QWs with different thickness located at different distance from the processed surface. In particular we studied two types of growth interruptions before the deposition of the QWs: in-situ process (under an UHV environment), and ex-situ process (with air exposure). We present results of the change in the QWs interfacial roughness and its correlation with the specific process performed at the interfaces.

2. Experimental Details

The samples investigated here consisted of three GaAs/AlGaAs QWs with nominal well thickness of 60, 45, and 25 Å. A schematic illustration of the samples structure is shown in the inset of Fig. 1. The QWs were grown by MBE on (100) oriented GaAs substrates at a temperature of 600°C using the following growth sequence:

1. Growth of a 5000 Å thick $Al_{0.3}Ga_{0.7}As$ layers to smooth out the GaAs substrate surface imperfections.
2. Growth of a GaAs buffer layer of thickness *d*. The growth interruption was performed on the surface of this buffer layer.
3. In-situ / ex-situ growth interruption. The characteristics of this process for each sample are explained below.
4. Growth of the first $Al_{0.3}Ga_{0.7}As$ barrier with a thickness of 200 Å.
5. Deposition of three quantum wells QW_1, QW_2, and QW_3, with nominal thickness of 60, 45, and 25 Å, separated with 400 Å- thick $Al_{0.3}Ga_{0.7}As$ barriers, respectively.
6. Growth of the last $Al_{0.3}Ga_{0.7}As$ barrier with a thickness of 1000 Å. None of the layers was intentionally doped.

In order to study the effects of a growth interruption performed under an UHV environment (in-situ interruption), and those of a process involving air exposure (ex-situ interruption), we designed two different sets of samples. For samples #1 and #2, during the step 3 the samples were taken out of the MBE system, the GaAs surface with a reconstruction (2x4) was exposed to air for a period of 30 min, and then introduced back to the MBE system to continue with the QWs growth. The thickness *d* of the air exposed GaAs buffer layer was 5000 and 500 Å for samples #1 and #2, respectively. For samples #3 and #4 the growth was interrupted after the deposition of a thin GaAs buffer layer of thickness *d*=130 Å. In order to study the effects of the growth interruption on GaAs layers with different surface reconstructions, we prepared the surface of the buffer layer with the reconstruction (2x4) and c(4x4), for samples #3 and #4, respectively. The GaAs surface reconstructions were determined by reflection high-energy electron diffraction (RHEED). The samples were taken out of the MBE chamber, moved without air-exposure to a transfer chamber through UHV tunnels, and maintained there for 3 hours in a 10^{-9} Torr UHV environment. Then the samples were transferred back to the MBE chamber to continue with the QWs growth. The characteristics of the ex-situ and in-situ interrupted samples were compared with those of a reference sample (sample #0), which has in the step 2 a GaAs layer of thickness *d*= 5000Å. The three QWs were continuously grown, no interruption was made whatsoever on this sample. The characteristics and process performed in each sample are summarized in Table 1.

PL measurements were performed employing a standard set up. The PL spectra were recorded with the samples mounted on a cold finger with continuos–flow of liquid Nitrogen (77 K). The samples were excited with an Ar laser (λ= 6320 Å).

3. Results and discussion

Fig. 1 and 2 show PL spectra at 77 K from the studied samples. First we will discuss the PL spectrum features of the reference sample (sample #0) shown in Fig. 1(a). We clearly observe four peaks in the spectrum at energies of 1.507, 1.589, 1.633 and 1.722 eV, respectively. The energy position of the band-to-band transition from bulk GaAs is given by the Varshni relation:

$$E_g(T) = E_g(0) - \frac{\alpha T^2}{\beta + T} \quad (1)$$

For GaAs α= $5.5x10^{-4}$ eV/K and β= 225 K. From this equation at 77 K we obtain an energy of 1.505 eV. This

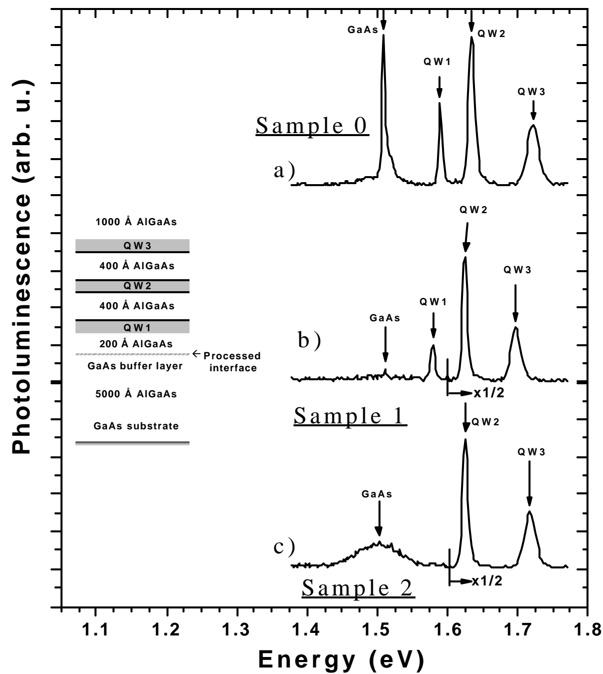

Figure 1. Photoluminescence spectra at 77 K of the reference and the two different ex-situ processed samples. The inset shows a schematic figure of the samples structure.

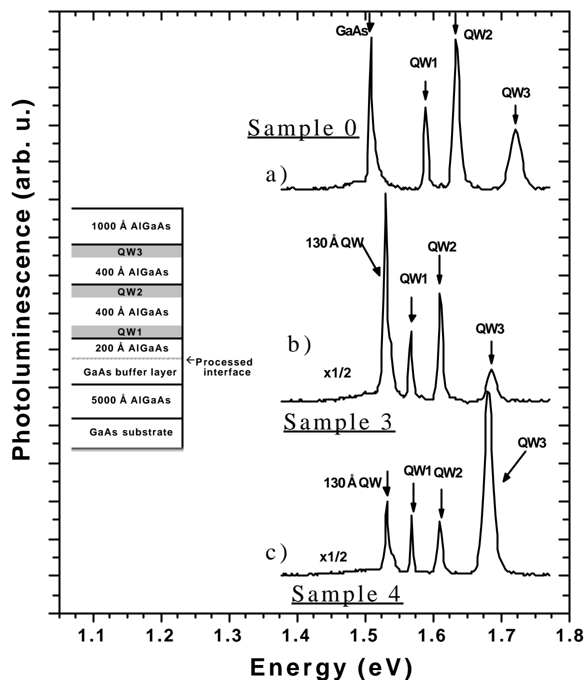

Figure 2. Photoluminescence spectra at 77 K of the reference and the two different in-situ processed samples. The inset shows a schematic figure of the samples structure.

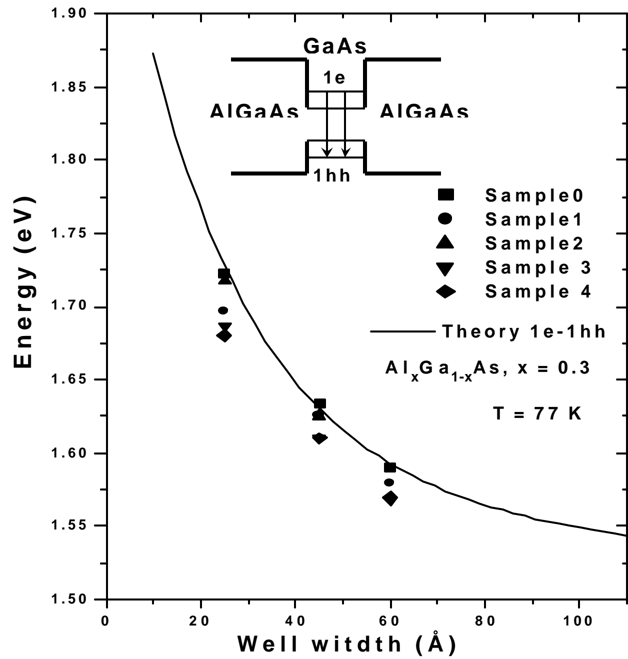

Figure 3. Energy position of the PL peaks associated to QW_1, QW_2, and QW3 in the different samples. The line was obtained from a theoretical model of a finite quantum well, as shown in the in-set.

value is very close to the position of the first peak at 1.507 eV in Fig 1(a), therefore we assign this peak to the emission from the 5000 Å-thick GaAs buffer layer.

The other three peaks marked with QW_1, QW_2, and QW_3, in the spectrum of Fig. 1(a) are associated to the emission from the quantum wells. In order to calculate the energy position expected from the QWs emission we solved the Schrödinger equation for a finite barrier QW (see inset Fig. 3), taking into account the discontinuity in the effective mass as the carriers go from the $Al_{1-x}Ga_xAs$ barrier to the GaAs well [14]. From this model we obtained the energy position as a function of the well width, expected in the recombination from the first electron-heavy hole transition (1e-1hh) in the QWs, the result is shown by the continuous line in Fig. 3. According to this model the emission from QWs with nominal thickness of 25, 45, and 60 Å should be at energies of 1.727, 1.630 and 1.593 eV, respectively. These theoretical values are very close to the energy positions of the peaks marked with QW_1, QW_2, and QW_3 in the PL spectrum of Fig. 1(a), thus confirming that these peaks are associated to the 1e-1hh transitions in the quantum wells.

In order to further analyze the PL spectrum from sample #0, each one of the peaks associated to the QWs was fitted to a gaussian function. From the full width at half maximum (FWHM) of the gaussian functions we can estimate the uncertainty (ΔL) associated to statistical variations in the well width (roughness at the interfaces as

illustrated in the inset of Fig. 4), by using the following equation [8]:

$$\Delta E = \left[\left(\frac{dE_{1e}}{dL} \right) + \left(\frac{dE_{1hh}}{dL} \right) \right] \Delta L \qquad (2)$$

with:

$$\left(\frac{dE_{1e}}{dL} \right) = \frac{E_{1e}}{\frac{L}{2} + \frac{\hbar \Delta E_C}{E_{1e}\sqrt{2m_e^B(\Delta E_C - E_{1e})}} Cos^2\left(\frac{L}{2}\sqrt{\frac{2m_e^W}{\hbar^2}E_{1e}} \right)}$$

$$\left(\frac{dE_{1hh}}{dL} \right) = \frac{E_{1hh}}{\frac{L}{2} + \frac{\hbar \Delta E_V}{E_{1e}\sqrt{2m_{hh}^B(\Delta E_V - E_{1hh})}} Cos^2\left(\frac{L}{2}\sqrt{\frac{2m_{hh}^W}{\hbar^2}E_{1hh}} \right)}$$

Where ΔE is the FWHM of the involved transition, L is the well width, E_{1e}, E_{1hh} are the energy values of the 1e and 1hh levels. m_e^W, m_{hh}^W, m_e^B, m_{hh}^B are the effective mass of the electron and heavy hole in the well (W) and barrier (B), ΔE_C, ΔE_V are the discontinuities at the conduction and valence band, respectively. These parameters were obtained from ref [15].

The results for sample #0 are shown by solid squares in Fig. 4. The uncertainty ΔL associated to QW_1 and QW_2 is around 1 ML, and decreased to 0.8 ML for the QW_3.

Now we present the results of the integrated PL intensity associated to the QWs in sample #0. The integrated PL intensity for each QW was obtained from the area of the gaussian functions obtained from the fittings to the PL peaks. The results are shown in Fig. 5 as solid

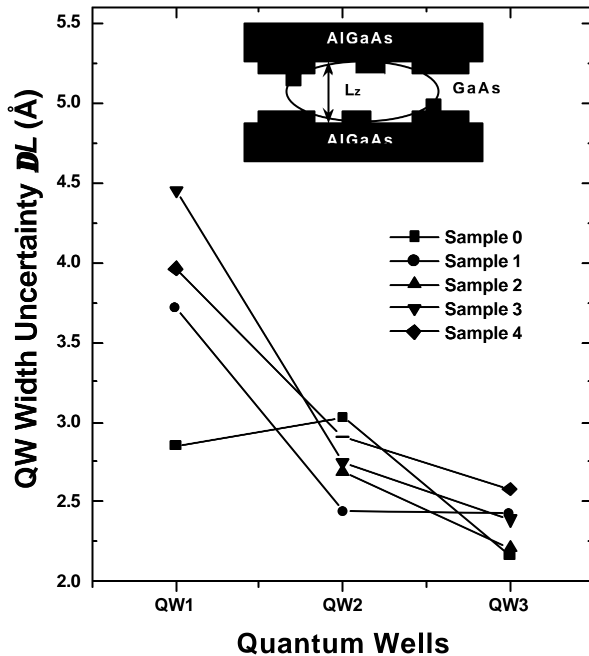

Figure 4. Interface roughness associated to QW_1, QW_2, and QW3 for the different samples. The inset show a schematic picture of the QWs interfaces employed to calculate the roughness.

squares. We note that for sample #0 the most intense emission is associated to QW_2. In order to explain this particular distribution in the PL intensity different factors should be taken into account like: excitation power and energy, different trapping cross sections of the QWs, carrier diffusion, etc., but considering all these factors is out of the scope of the present paper. Here we will focus on the changes in the PL spectra associated to the different types of growth interruptions, taking as the reference from non-interrupted MBE grown QWs the spectrum of sample #0.

Next we will discuss the PL spectra shown in Fig. 1(b) and (c) from samples #1 and #2 that were ex-situ interrupted. We observe drastic changes in the PL spectra induced by the growth interruption. First we note a shift to lower energies in the PL peaks position associated to the emissions from the QWs. The energy positions of the PL peaks associated to the QW_1, QW_2, and QW_3 are plotted in Fig. 3 as circles and triangles, for samples #1 and #2, respectively. According to the above discussed theoretical model, these red shifted emissions should correspond to thicker QWs than those intended to grow. We think that the thicker QWs are the result of the long period of time that the source cells were closed during the growth interruption. When opening the cells shutters to re-start the growth, transient instabilities of the beam fluxes [16] may cause an increase of the growth rate resulting in the deposition of thicker QWs.

In the spectrum of sample #2 the transitions from the thin 500 Å GaAs buffer layer and that from the first QW are not well defined, resulting in a very broad emission centered at about 1.51 eV. This clearly shows that the ex-situ growth interruption strongly affects the quality of the air-exposed GaAs buffer layer, and that the effects extend up to the QW_1. The quality deterioration is associated to the introduction of impurities [17], and non-radiative recombination centers [18] during the air-exposure resulting in wide and low intensity PL peaks. It is interesting to note that by increasing the thickness of the air-exposed GaAs buffer layer to 5000 Å (sample #1), the emission from this layer and that from the QW_1 become more defined. As observed in Fig. 1(b), the peak at 1.5 eV associated to the 5000 Å GaAs layer is clearly observed, although still with very low intensity that reflects non-radiative recombination of carriers at the air-exposed GaAs surface. The PL peak associated to the QW_1 presented a recovered intensity, but was wider than that of sample #0 indicating roughening at the AlGaAs/GaAs interfaces induced by the ex-situ growth interruption. The PL peaks associated to the transitions in QW_2 and QW_3, for both samples #1 and #2, presented strong and narrow emissions indicating that the air-exposed induced damage was totally buried after the growth of a few hundreds of amstrongs.

Next we will present the results of the in-situ interrupted samples. Fig. 2(b) and (c) show the PL spectra of samples #3 and #4, respectively. The energy positions of the PL peaks associated to the three QWs are plotted in Fig. 3 as inverted triangles and diamonds, for samples #3 and

#4, respectively. As in the ex-situ interrupted samples, the PL peaks position corresponding to the QWs are shifted to lower energies, as above explained these red shifts are associated to beam flux instabilities during the first minutes after opening the source cells shutters. An important difference of the PL spectra in Figs. 2 (b) and (c) is that the emission corresponding to the GaAs buffer layers is shifted to higher energies. This blue shift is due to the small width of 130 Å used for the buffer layers in the in situ interrupted samples. In fact, this thin layer is acting as a thick quantum well, its PL emission at 1.53 eV is associated to a QW of thickness of 135 Å, that is very close to the nominal thickness. It is also important to note that, despite the smaller width, the PL intensity from the GaAs buffer layers in the in-situ interrupted samples is much higher than that corresponding to the ex-situ interrupted samples. This shows the great advantage of UHV-processing methods over techniques requiring air-exposure. Another interesting result from Figs. 2(b) and (c), is that the buffer layer with a 2x4 surface reconstruction (sample #3) presented a more intense PL than that of the buffer layer with a c(4x4) surface reconstruction (sample #4). Thus indicating that the use of a GaAs surface terminated with the 2x4 reconstruction is better for in-situ processing purposes. Concerning the PL intensity from the QWs, we observe in Figs. 2(b) and (c) that all the PL peaks associated to the QWs are intense, including that of QW_1, which is the closest to the interrupted surface. Sample #3 has the PL spectrum shape that most resemble that of the reference sample #0. The PL spectrum of sample #4, presented strong changes in the PL intensity distribution among the QWs, this point will be discussed below.

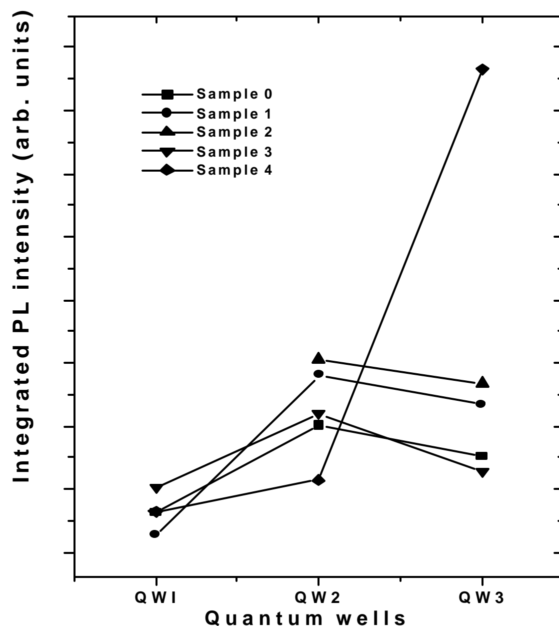

Figure 5. Integrated photoluminescence intensity associated to QW_1, QW_2, and QW3 for the different samples.

The roughness and PL intensities of the QW_1, QW_2, and QW_3 in all the studied samples are summarized in Figs. 4 and 5, respectively. From Fig. 4 we observe that in general, both in-situ or ex-situ interruptions induced roughness in the QW_1, the closest to the processed interface. However, in all the processed samples the roughness decreased for the QW_2 and QW_3, this indicates an improvement in the crystal quality moving away from the interrupted surface as the growth proceeds. From Fig. 5 we note that among all the QW_1 in the different samples, those in the ex-situ processed samples presented the lowest PL intensities. This is caused by the introduction of a large amount of non-radiative recombination centers during the air-exposure [19,20]. Sample #3 presented the highest PL intensity for the QW_1, indicating the high quality obtained with an in-situ interruption of a 2x4 GaAs surface. It is interesting to note that although the first QW is severely damaged in the ex-situ interrupted samples, the QW_2, and QW_3 presented strong PL intensities. We also observe in Fig. 5 a very strong emission from QW_3 in sample #4. As previously stated, the PL intensity distribution among the QW_1, QW_2, and QW_3 strongly depends on the photoexcited carriers diffusion along the different layers in each sample. The presence of internal electric fields in the samples is expected to change the carriers diffusion process, and thus the way each QW emits light. It has been reported that a growth interruption process introduces a high density of impurities and interfacial states [17-20], causing strong built-in internal electric fields in the epitaxial layers [21]. Thus, we think that the above described peculiar PL intensity distributions in samples #1, #2, and #4 are caused by different internal electric fields generated by the different growth interruptions. Sample #3 presented a PL intensity distribution in the QWs very similar to that of the reference sample, suggesting low built-in internal electric fields in this sample. The differences found between sample #3 and #4, suggest us that the incorporation of impurities from the residual background pressure is sensitive to GaAs surface reconstruction during the in-situ interruption.

4. Conclusions

We have performed ex-situ (with air-exposure), and in-situ (under UHV-environment) growth interruptions on GaAs buffer layers grown by MBE. Three AlGaAs/GaAs QWs were grown on the processed GaAs surfaces, the effects of the different growth interruptions on the GaAs buffer layer and QWs properties were studied by photoluminescence spectroscopy. Ex-situ interrupted samples showed degraded PL characteristics in the buffer layer and in the QW nearest to the processed interface indicating a great induced damage. In contrast, in-situ interrupted samples presented little induced damage, in particular the sample interrupted with a GaAs 2x4 surface reconstruction presented the best PL properties. This result provides important information to chose the best GaAs surface termination for in-situ processing purposes.

Additionally, we observed strong changes in the distribution of PL intensity among the three QWs for the different samples, we associate these changes to different carriers diffusion processes induced by built-in internal electric fields generated by interfacial states or impurities incorporated during the growth interruption.

Acknowledgments

The authors acknowledge the technical support of A. Guillén-Cervantes, Z. Rivera-Alvarez, and Erasmo Gómez. This work was partially supported by CONACyT-México.

References

[1] D. Gammon, B. V. Shanabrook, and D. S. Katzer, Phys. Rev. Lett. **67**, 1547 (1991).
[2] C. Weisbuch, R. C. Miller, R. Dingle, A. C. Gossard, and W. Weigmann, Solid State Commun. **37**, 1550 (1981).
[3] D. Bimber, F. Heinrichsdorff, R. K. Bauer, D. Gerthsen, D. Stenkamp, D. E. Mars, J. N. Miller, J. Vac. Sci. Technol. B. **10**, 1793 (1992).
[4] J. V. D. Veliadis, J. B. Khurgin, Y. J. Ding, A. G. Cui, D. S. Katzer, Phys. Rev. B 50, 4463 (1994).
[5] S. Hiyamizu, S. Shimomura, A. Wakejima, S. Kaneko, A. Adachi, Y. Okamoto, N. Sano, K. Murase, J. Vac. Sci. Technol. B. **12**, 1043 (1994).
[6] K. Ploog, A. Fisher, L. Tapfer, and B. F. Feuerbacher, J. Cryst. Growth **111**, 344 (1991).
[7] M. Tanaka, H. Sakaki, J. Yoshino, and T. Furata, Surf. Sci. **174**, 65 (1986).
[8] M.A. Herman, D. Bimberg, and J. Christen, J. Appl. Phys.**70**, R1 (1991).
[9] K. Brunner, G. Abstreiter, G. Böhm, G. Tränkle, and G. Weimann, Appl. Phys. Lett. **64**, 3320 (1994).
[10] B. Orschel, G. Oelgart, ands R. Houdré, Apply. Phys. Lett. **62**, 843 (1993).
[11] T. Ishikawa and M. López, Int. J. Mod. Phys. B **10**,3637 (1996).
[12] M. Hong, J. Cryst. Growth **150**, 277 (1995).
[13] S. Guel-Sandoval, A. H. Pastón, Swaminathan, T. Srinivasan, S.H. Sun, S. D. Hersee, M. S. Allen, C. E. Moeller, D. J. Gallant, G. C. Dente, J. G. McInerny, Appl. Phys. Lett. **66**, 2048 (1995).
[14] G. Bastard: *Wave Mechanics Applied to Semiconductor Heterostructures* (Les Editions de Physique, France, 1988).
[15] L. Paresi, M. Guzzi, J. Appl. Phys. **75**, 4779 (1994).
[16] P. A. Maki, S. C. Palmateer, A. R. Calawa, and B. R. Lee, J. Vac. Sci. Technol. B. **4**, 564 (1986).
[17] R. C. Miller, C. W. Tu, S. K. Sputz, and R. F. Kopf, Appl. Phys. Lett. **49**, 1245 (1986).
[18] F. Wakaya, T. Matsubara, M. Nakayama, J. Yanagisawa, Y. Yuba, S. Takaoka, K. Murase, K. Gamo, J. Vac. Sci. Technol. B. **16**, 2313 (1998).
[19] M. López López, M. Meléndez, and S. Goto., Appl. Phys. Lett. **71**, 338 (1997).
[20] S. Kohmoto, Y. Nambu, K. Asakawa, and T. Ishikawa, J. Vac. Sci. Technol. B **14**, 3646 (1996).
[21] M. López-López, J. Luyo-Alvarado, M. Meléndez-Lira, O.Cano-Aguilar, C.Megía-García, J. Ortiz-López, and G. Contreras-Puente, J. Vac. Sci. Technol B **18**, 1553 (2000).